BIOCHEMISTRY
including biophysical chemistry & molecular biology
Article

Biochemistry **2009,** *48,* 4691–4698 4691
DOI: 10.1021/bi900092w

Effects of Polyamines on the DNA-Reactive Properties of Dimeric Mithramycin Complexed with Cobalt(II): Implications for Anticancer Therapy[†]

Ming-Hon Hou,*[,‡,§,∥] Wen-Je Lu,[‡] Chun-Yu Huang,[‡] Ruey-Jane Fan,[‡,§] and Jeu-Ming P. Yuann[⊥]

[‡]*Biotechnology Center and* [§]*Institute of Genomics and Bioinformatics and* [∥]*Department of Life Science, National Chung Hsing University, Taichung, 402 Taiwan, and* [⊥]*Department of Biotechnology, Ming Chuan University, Taoyuan County, 333 Taiwan*

Received January 21, 2009; Revised Manuscript Received April 12, 2009

ABSTRACT: Few studies have examined the effects of polyamines on the action of DNA-binding anticancer drugs. Here, a Co(II)-mediated dimeric mithramycin (Mith) complex, $(Mith)_2$−Co(II), was shown to be resistant to polyamine competition toward the divalent metal ion when compared to the Fe(II)-mediated drug complexes. Surface plasmon resonance experiments demonstrated that polyamines interfered with the binding capacity and association rates of $(Mith)_2$−Co(II) binding to DNA duplexes, while the dissociation rates were not affected. Although $(Mith)_2$−Co(II) exhibited the highest oxidative activity under physiological conditions (pH 7.3 and 37 °C), polyamines (spermine in particular) inhibited the DNA cleavage activity of the $(Mith)_2$−Co(II) in a concentration-dependent manner. Depletion of intracellular polyamines by methylglyoxal bis(guanylhydrazone) (MGBG) enhanced the sensitivity of A549 lung cancer cells to $(Mith)_2$−Co(II), most likely due to the decreased intracellular effect of polyamines on the action of $(Mith)_2$−Co(II). Our study suggests a novel method for enhancing the anticancer activity of DNA-binding metalloantibiotics through polyamine depletion.

Polyamines (e.g., spermine and spermidine) are ubiquitous cellular constituents that play important biological roles in cell growth and differentiation (*1*, *2*). Intracellular polyamines are present in the millimolar (mM) range (*1*). In cancer cell lines, polyamine metabolism is frequently dysregulated, leading to higher polyamine concentrations than in normal cells (*3*, *4*). The inhibition of polyamine biosynthesis by polyamine inhibitors such as 2-difluoromethylornithine (DFMO)[1] is a potential avenue for cancer chemotherapy (*5*). Due to the protonation of the amine groups, polyamines bear multiple positive charges (i.e., two for putrescine, three for spermidine, and four for spermine) at physiological pH values. Polyamines are almost exclusively bound to nucleic acids via nonspecific electrostatic interactions and are involved in many cellular processes that require nucleic acids (*6*, *7*). Moreover, a previous study showed that the polyamine binding sites are located within both the major and minor DNA grooves (*8*−*10*). The binding of polyamines to DNA removes the difference in stability among various DNA structures, whose interconversion can then be carried out with minimal energy barriers. This may have relevance in the possible biological functions associated with DNA polymorphisms (*11*).

Mithramycin (plicamycin, Mith) is a member of the aureolic family of drugs isolated from *Streptomyces plicatus* and contains A-B disaccharide and C-D-E trisaccharide moieties that are connected to a chromophore aglycon via opposing O-glycosidic bonds (*12*) (Figure 1). This drug has been used clinically to treat several types of cancer including testicular carcinoma, chronic myeloid leukemia (CML), and acute myeloid leukemia (AML) (*13*, *14*). Structural analysis revealed that Mith binds to the minor groove of DNA duplexes around GC-rich sequences and that this binding is mediated by divalent metal ions such as Mg(II), Co(II), and Fe(II) (*15*−*17*). These metal ions have octahedral coordination geometry and bind to O1 and O9 atoms of the two chromophores, while two water molecules act as the fifth and sixth ligands. The effects of metal ions on the DNA-binding properties of the aureolic family drugs have been discussed previously (*18*, *19*). The activity of the metal derivative complex of Mith against cancer is associated with DNA-binding affinity and DNA cleavage activity (*18*−*20*). Polyamines have been reported to protect against DNA damage caused by agents such as ionizing radiation and reactive oxygen species (*21*−*25*). Moreover, previous studies have shown that polyamines are able to interact with transition metals such as Fe(II), Cu(II), and Zn (II) (*26*), possibly by affecting the coordination between the divalent metal ion and the drug in the metal-derived complex. Nevertheless, little is known about polyamine effects on the action of DNA-binding anticancer drugs.

The metals Co and Fe have redox-cycling activity and have been widely utilized in the development of DNA-acting metalloantibiotics (*27*). In this study, we found that Co(II), but not Fe (II), was resistant to polyamine competition in the formation of a dimeric Mith complex, $(Mith)_2$−Co(II), with and without DNA

[†]This work was supported by the NCS 95-2311-B-005-015-MY2 (to M.-H.H.).

*To whom the correspondence should be addressed at the Institute of Genomics and Bioinformatics, National Chung Hsing University. Tel: 886-4-22840450 ext 6131. Fax: 886-4-22861905. E-mail: mhho@dragon.nchu.edu.tw.

[1]Abbreviations: Mith, mithramycin; MGBG, methylglyoxal bis(guanylhydrazone); CD, circular dichroism; SPR, surface plasmon resonance; K_a, association equilibrium constant; K_d, dissociation equilibrium constant; k_a, association rate constant; k_d, dissociation rate constant; DFMO, 2-difluoromethylornithine.

Published on Web 04/15/2009

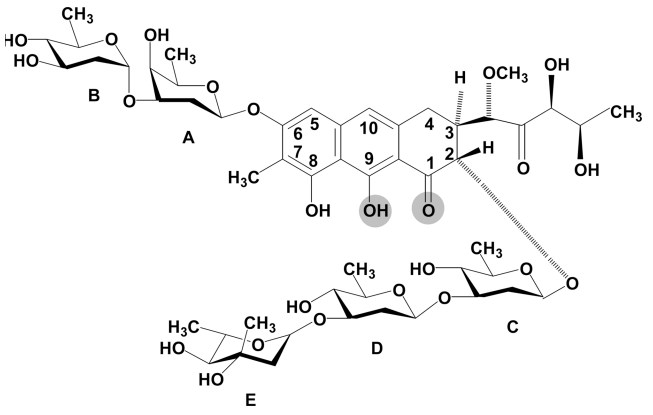

FIGURE 1: Chemical structure of mithramycin (Mith). The oxygen atoms that coordinate the metal ion are shaded.

binding of this complex. Our results characterized the effects of polyamines on the DNA-reactive properties and cytoxicity of $(Mith)_2$−Co(II) and suggest a novel method for anticancer therapy through polyamines depletion.

EXPERIMENTAL PROCEDURES

Mithramycin, MGBG, spermine, and spermidine were purchased from Sigma Chemical Co. (St. Louis, MO). Absorbance measurements were carried out in a quartz cuvette using a Hitachi U-2000 spectrophotometer. The concentrations of Mith were estimated using an extinction coefficient of 10000 M^{-1} cm^{-1} at 405 nm (*18*). The concentrations of oligonucleotides were determined according to Beer's law ($A = \varepsilon bc$, where A is the optical density at 260 nm, ε is the extinction coefficient, b is the cell path length (1 cm), and c is the DNA concentration in molar). The extinction coefficient of plasmid DNA is 6600 M^{-1} cm^{-1}. Synthetic DNA oligonucleotides were purified by gel electrophoresis. Oligomer extinction coefficients were calculated according to tabulated values of monomer and dimer extinction coefficients with reasonable assumptions (*28*).

Circular Dichroism (CD) Experiments. CD spectra were collected between 520 and 200 nm with bandwidth at 1 nm intervals using a JASCO-815 spectropolarimeter. Temperature was controlled by a circulating water bath. All spectra consisted of the average of three runs. The methods for the CD spectral analyses have been described previously (*11*, *29*). The molar ellipticity $[\theta]$ was calculated from the equation $[\theta] = \theta/Cl$, where θ is the relative intensity, C is the molar concentration of oligonucleotides, and l is the path length of the cell in centimeters.

Surface Plasmon Resonance (SPR) Binding Analysis. The affinity between the drug and DNA duplexes was measured in a BIAcore 3000A SPR instrument (Pharmacia, Uppsala, Sweden) with a SensorChip SA5 (Pharmacia) by monitoring the refractive index change of the sensor chip surface. These changes are generally assumed to be proportional to the mass of the molecules bound to the chip and are recorded in resonance units (RU). 5′-Biotin-labeled hairpin DNA duplexes, 5′-TTTTGGCCAATGTTTGGCCAA-3′, purified by PAGE were used in the SPR experiments. To control the amount of the DNA that bound to the streptavidin SA chip surface, the biotinylated oligomer was immobilized manually onto the surface chip. The metal derivative complexes of Mith were prepared in a solution of 20 mM Tris-HCl (pH 7.3), 50 mM NaCl, and polyamines at various concentrations. Different concentrations of complexes were passed over the chip surface for 180 s at a flow rate of 10 μL min^{-1} to reach equilibrium, and one of the flow cells was kept blank as a control. The blank buffer solution was then passed over the chip to initiate the dissociation reaction, and this flow was continued for an additional 300 s to complete the reaction. The surface was then recovered by washing with 10 μL of 10 mM HCl. Analyses of the SPR-binding constants have been described previously (*11*). Sensorgrams for the interactions between hairpin DNA duplexes and drugs were analyzed using BIA evaluation software, version 3. The fitting was accepted when χ^2 values were lower than 3.

Measurement of DNA Strand Breakage Using Plasmid DNA. *Escherichia coli* were transformed with pGEM-7Zf(−) and grown in LB medium. The plasmid DNA was then purified using a Qiagen plasmid purification kit (Valencia, CA). Reagents were added in the following order: phosphate buffer (pH 7.3), $(Mith)_2$−Co(II), supercoiled plasmid DNA, and H_2O_2 (note that phosphate, not Tris, buffer was used for the analysis of DNA strand breakage, because Tris has been previously shown to generate formaldehyde upon reaction with hydroxyl radicals (*30*)). Polyamines were coincubated as indicated. The samples were incubated at 37 °C for 30 min, and the reactions were stopped with thiourea prior to electrophoresis in a 1% agarose gel, which was followed by ethidium bromide staining for analysis. Densitometry of the DNA bands on the gel was achieved using Uniphoto Band Tool software.

Cell Viability and Intracellular Polyamine Concentration Assay. The human alveolar epithelial carcinoma cell line A549 was kindly provided by Dr. Kuan-Chih Chow (Institute of Biomedical Science, National Chung Hsing University). Cells were grown in RPMI-1640 medium containing 10% fetal bovine serum (FBS), 1% L-glutamine, 1% penicillin/streptomycin, and 25 mM HEPES and maintained at 37 °C in a humidified atmosphere containing 5% CO_2 and 95% air. For cell viability assays, cells were seeded into 24-well culture plates at a density of 1×10^5 cells. Cell viability was evaluated by the MTT (dimethylthiazole diphenyltetrazolium bromide; thiazolil blue) assay. MTT is a water-soluble tetrazolium salt that yields a yellowish solution when prepared in phenol red-free (RPMI) medium. Dissolved MTT is converted into insoluble purple formazan when active mitochondrial dehydrogenases of living cells cleave the tetrazolium ring. Cells were incubated with or without 1 μM MGBG for 24 h. Thereafter, the MGBM-containing solution was washed out and replaced with a solution containing various concentrations of $(Mith)_2$−Co(II) or the vector control for another 24 h. Subsequently, the MTT solution (500 μg/mL medium, final concentration) was added to each well; the added volume was normalized to one-tenth of the original culture medium volume, and cells were then incubated at 37 °C for 2 h. The solution was removed, and 2-propanol was added to solubilize the stain. The results were evaluated using a SpectraMax M2 plate reader (Molecular Devices, Sunnyvale, CA), which yielded the absorbance intensity as a function of the viable cell number. The cell viability assay results were expressed as the standard error of the mean (SEM), $S_X = S/n^{1/2}$, where S is the standard deviation and n is the number of experiments. The mean values were compared using a two-way analysis of variance (ANOVA) test (SigmaStat v2; SPSS Inc., Chicago, IL). The level set for statistical significance was $p < 0.05$.

Intracellular polyamines were extracted with 3% perchloric acid (v/v). The supernatant was used for dansylation with dansyl chloride in acetone. The dansyl amides were extracted with toluene and separated by a thin-layer chromatography (TLC)

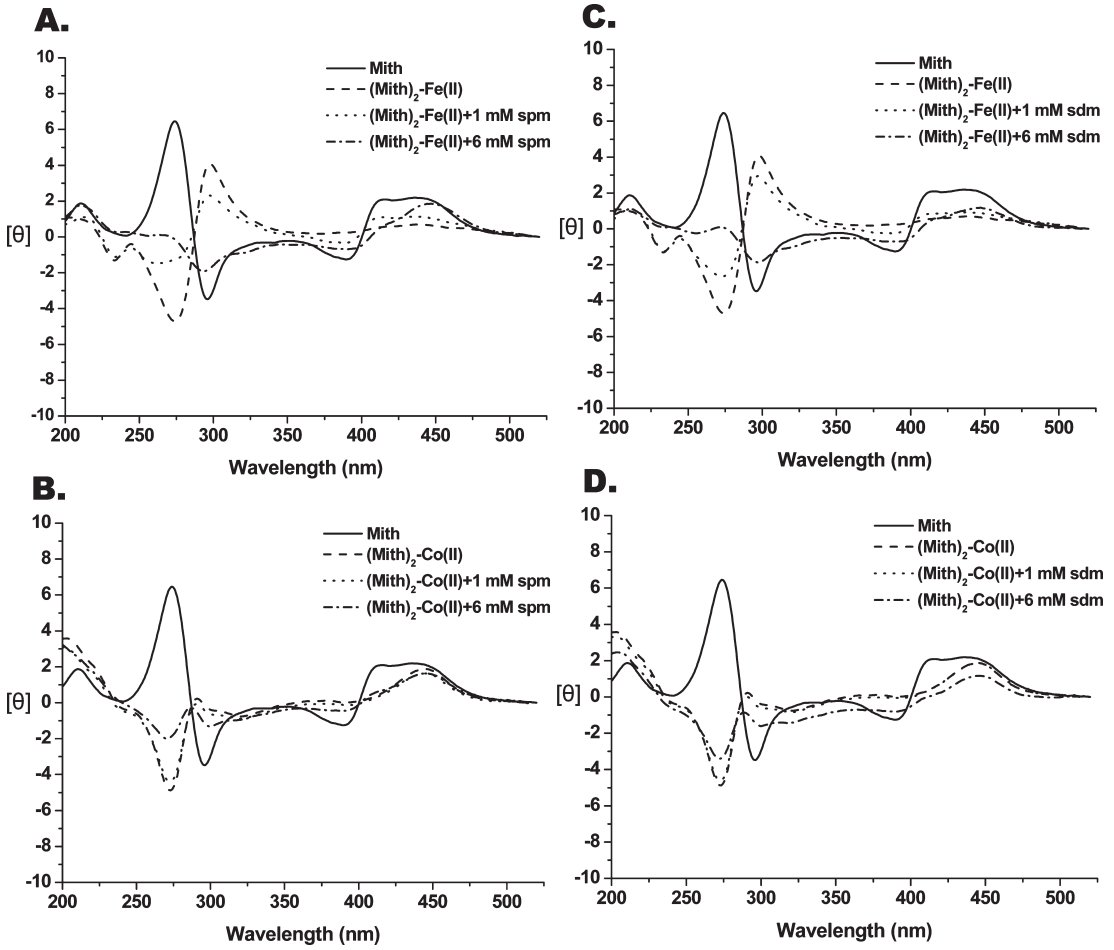

FIGURE 2: Comparison of the CD spectra of Mith, dimeric Mith−complexed metal ion(II), and the dimeric complex in the presence of (A, B) spermine (spm) and (C, D) spermidine (sdm) at 1 and 6 mM at 20 °C. The metal ions(II) include Fe(II) and Co(II). The drug concentration was 0.04 mM in a buffer of 20 mM Tris-HCl (pH 7.3).

plate using a mobile phase of ethyl acetate/cyclohexane (2:3 v/v). The intensity was quantified by a spectrophotometer with excitation and emission at 365 and 505 nm, respectively.

RESULTS

Effects of Polyamines on the Structural Integrity of (Mith)$_2$−Fe(II) and (Mith)$_2$−Co(II). The effects of polyamines on the structural integrity of (Mith)$_2$−Fe(II) and (Mith)$_2$−Co(II) were monitored using CD spectroscopy. As shown in Figure 2, the CD spectra of (Mith)$_2$−Fe(II) and (Mith)$_2$−Co(II) were scanned from 200 to 520 nm in the presence of increasing concentrations (0, 1, and 6 mM) of spermine or spermidine. The intensity at ~275 nm is indicative of a transition between the monomers and dimers of the aureolic family drugs, based on our previous studies (*18*, *19*). The CD spectra of the Mith monomer showed an obvious positive peak at 275 nm, and an inversion of the peak was observed during the formation of (Mith)$_2$−Fe(II) and (Mith)$_2$−Co(II) (Figure 2). In the presence of 1 mM spermine or spermidine, the CD spectrum intensity of (Mith)$_2$−Fe(II) at 275 nm was decreased, while the intensity of (Mith)$_2$−Co(II) remained at the same level, suggesting that the structural integrity of (Mith)$_2$−Co(II) was not affected. When 6 mM spermine or spermidine was added, the negative peak of the (Mith)$_2$−Fe(II) CD spectrum reverted to a small broad positive peak, which suggests that more than half of (Mith)$_2$−Fe(II) reverted to the monomer form. On the other hand, the negative peak of CD spectrum of (Mith)$_2$−Co(II) at 275 nm was changed (θ = ~3 or 1.5) in the presence of 6 mM spermine or spermidine, respectively. However, at these polyamine concentrations, the CD spectra of (Mith)$_2$−Co(II) mostly maintained a negative shape at 275 nm, suggesting that the dimer conformation of (Mith)$_2$−Co(II) were predominately preserved. These results suggest that (Mith)$_2$−Co(II) is more resistant to polyamine competition for Co(II), compared with the (Mith)$_2$−Fe(II) complex in the absence of a DNA duplex.

Effects of Polyamines on the Structural Integrity of (Mith)$_2$−Fe(II) and (Mith)$_2$−Co(II) during DNA Duplex Binding. In order to characterize the effects of polyamines on the structural integrity of (Mith)$_2$−Fe(II) and (Mith)$_2$−Co(II) while interacting with DNA, these complexes were allowed to interact with hairpin DNA duplexes in the presence of increasing concentrations (0, 1, and 6 mM) of spermine or spermidine and monitored by CD spectroscopy. The test DNA, 5′-TTGGCCAATGTTTGGCCAA-3′, forms a hairpin duplex using 5′-TGT-3′ as the loop region and provides one Mith DNA-binding site (GGCC). In Figure 3, the solid line shows the CD spectrum recorded from DNA and the Mith monomer complex (DNA + Mith). In the presence of Fe(II) and Co(II), however, the CD spectral features were completely different from those of DNA + Mith. According to our previous study, the induced CD intensity changes at 287 and 275 nm were evidence for the relative binding affinities of the metal ion(II)-mediated dimeric Mith complex toward this DNA oligomer duplex (*18*, *19*).

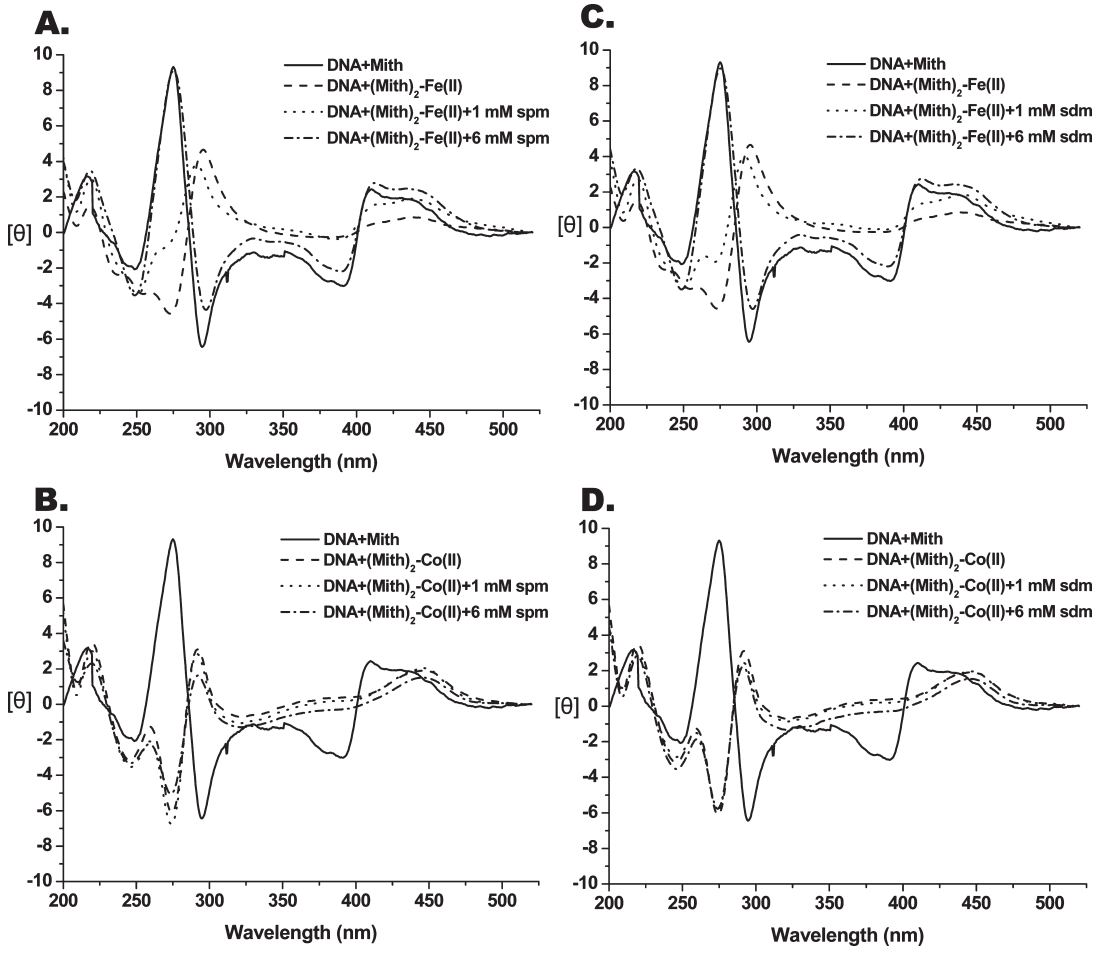

FIGURE 3: Comparison of the CD spectra of Mith−DNA, $(Mith)_2$−metal ion(II)−DNA, and $(Mith)_2$−metal ion(II)−DNA in the presence of (A, B) spermine (spm) and (C, D) spermidine (sdm) at 1 and 6 mM at 20 °C. Metal ions(II) include Fe(II) and Co(II). The drug concentration was 0.04 mM in a buffer of 20 mM Tris-HCl (pH 7.3).

When 1 mM spermine or spermidine was added, the CD spectrum intensities of $(Mith)_2$−Fe(II)−DNA at 275 and 287 nm were changed, signaling partial conversion of the dimer complex into drug monomer. In the presence of 6 mM spermine or spermidine, the CD spectrum of $(Mith)_2$−Fe(II)−DNA completely reverted to the same shape as DNA + Mith, implying that Fe(II) was completely removed by polyamines at high concentrations. Previous studies have shown that Fe(II) was able to bind to the negatively charged phosphate backbone and nitrogen bases in DNA (*31*). We suggest that DNA is involved in the competition between polyamines and $(Mith)_2$−Fe(II) by reacting with Fe(II), leading to complete disruption of this dimeric complex. On the other hand, the CD spectra of $(Mith)_2$−Co(II)−DNA complexes were basically identical in the absence and presence of polyamines, suggesting that $(Mith)_2$−Co(II) complexes are more resistant to the removal of Co(II) by polyamine competition during DNA binding.

Effects of Polyamines on the DNA-Binding Affinity of $(Mith)_2$−Co(II) Bound to Hairpin DNA Duplexes. To characterize the effects of polyamines on the binding affinity of $(Mith)_2$−Co(II) for DNA, complexes were allowed to interact with biotin-labeled hairpin DNA duplexes in the presence of spermine or spermidine, and the maximum binding capacity (R_{max}) (in RU) was measured by SPR. Biotin-labeled hairpin DNA duplexes were used as the probe and provided one Mith DNA-binding site (GGCC) with the trinucleotide 5′-TGT-3′ as the loop region. In Figure 4, the association between the hairpin DNA duplexes and $(Mith)_2$−Co(II) is shown by an increase in RU values (denoted A to B), whereas the dissociation of these two species was shown by a decrease on the same trace (denoted C to D). According to the SPR sensorgram, the interactions between the DNA duplexes and $(Mith)_2$−Co(II) exhibited the highest maximum capacity (~510 RU) in the absence of polyamines. Low concentrations of polyamines (1 mM) caused minor effects on the DNA-binding affinity of the complex. The affinity changed by only 20 RU in the presence of 1 mM spermine. Increasing the concentration of polyamines to 6 mM decreased the binding capacity of $(Mith)_2$−Co(II) and DNA. This was especially apparent with 6 mM spermine, which yielded the lowest (~135 RU) binding capacity.

Kinetic experiments were carried out by measuring the binding parameters between $(Mith)_2$−Co(II) and its target DNA duplex with or without polyamines. The kinetic constants of association (k_a in M^{-1} s^{-1}) and dissociation (k_d in s^{-1}) for $(Mith)_2$−Co(II) binding to hairpin DNA duplexes are based on the calculations from the association and dissociation phases of the SPR traces, respectively (Figure 4). The k_a value of $\sim 1.50 \times 10^4$ M^{-1} s^{-1} was essentially the same at low concentrations of polyamines. In the presence of 6 mM polyamines, however, the interactions between $(Mith)_2$−Co(II) and DNA had lower k_a values. The presence of 6 mM spermine resulted in a much lower k_a of 3.16×10^3 M^{-1} s^{-1}. The dissociation rate constants (k_d) of the buffer alone, 1 mM spermidine, 1 mM spermine, 6 mM spermidine, or 6 mM spermine were basically at the same level ($\sim 6 \times 10^{-2}$ s^{-1}), as

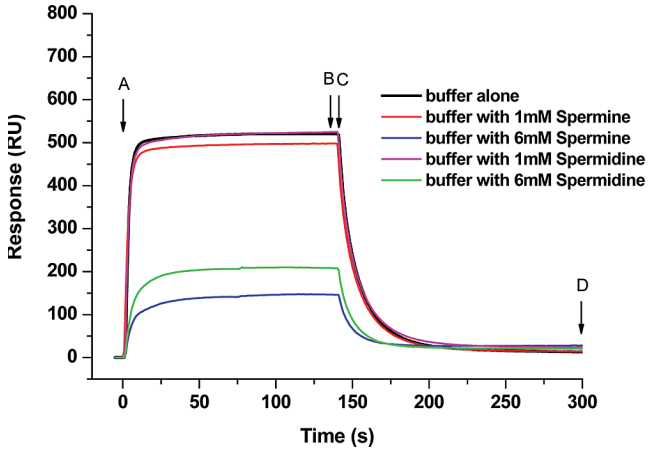

FIGURE 4: Sensorgrams of the interaction between an immobilized hairpin duplex and the target $(Mith)_2$−Co(II) (6 μM) in the presence of various concentrations of spermine and spermidine in a buffer of 20 mM Tris-HCl (pH 7.3) with 50 mM NaCl at 20 °C. The start (A) and end (B) points of the association and the start (C) and end (D) points of the dissociation are indicated by arrows.

shown in Table 1. These results suggest that polyamines mainly affected the binding of $(Mith)_2$−Co(II) to hairpin DNA duplexes in the association phase. The association constants (K_a) were calculated as k_a/k_d (in M^{-1}). As expected, polyamines at low concentrations showed higher K_a values in the interaction between $(Mith)_2$−Co(II) and DNA; K_a values were approximately 3- and 4-fold greater than those with 6 mM spermidine and spermine, respectively (Table 1).

Effects of Polyamines on the DNA Cleavage Activity of $(Mith)_2$−Co(II). To characterize the DNA cleavage properties of the $(Mith)_2$−Co(II) complex, plasmid DNA was treated with $(Mith)_2$−Co(II) (10 μM) in the presence of H_2O_2 at various time points as shown in Figure 5A. At 10 min, the supercoiled plasmid DNA was partially converted into an open circular form; at 30 min, the open circular form of plasmid DNA was further cleaved, resulting in linearization. These results suggest that the double-strand scissions formed during plasmid breakage by stepwise cleavage of the single strands. Moreover, after 120 min, the degradation of supercoiled DNA was almost complete, as shown by the appearance of smeared shorter DNA fragments. Figure 5B presents the results for plasmid DNA treated with $(Mith)_2$−Co(II) (10 μM) in the presence of H_2O_2 at various pH values after incubation for 30 min. At physiological pH (7.3), plasmid DNA was completely converted to its open circular and linear forms. At decreased pH (7.0−4.5), the amount of DNA in the open circular and linear forms was decreased, suggesting that the DNA cleavage activity of the complex was inhibited. Similarly to effects observed at pH 7.3, all plasmid DNA was present as one of the two cleavage products, the open circular and linear forms, at pH 8.3. However, in the pH range of 9.0−9.5, DNA degradation was inhibited as manifested by the appearance of supercoiled plasmid DNA. In addition, we characterized the effect of temperature on the DNA cleavage activity of the drug complex; at physiological temperature (37 °C), the linear form of plasmid DNA was observed (Figure 5C). Following a decrease in temperature, the DNA cleavage activity of the complex was decreased. All of these observations suggest that the physiological condition (pH 7.3 and 37 °C) is appropriate for the DNA cleavage activity of the complex.

To characterize the effect of polyamines on the DNA cleavage activity of $(Mith)_2$−Co(II), plasmid DNA was treated with $(Mith)_2$−Co(II) in the presence of H_2O_2 for 30 min with increasing concentrations (0, 1, 2, 5, and 10 mM) of spermine and spermidine as shown in panels A and B of Figure 6, respectively. In the absence of polyamines, supercoiled DNA was cleaved by $(Mith)_2$−Co(II) and converted into the open circular and linear forms. In the presence of spermidine or spermine at 1 mM, supercoiled DNA was also cleaved, suggesting that $(Mith)_2$−Co(II) maintained its DNA cleavage activity. In the presence of increasing concentrations of the polyamines, the amounts of open circular and linear plasmid DNA were diminished. At 2, 5, and 10 mM spermine, 84%, 27%, and 24% supercoiled DNA cleavage was observed, respectively, as compared to 98%, 73%, and 42% cleavage for spermidine at the same concentrations (Figure 6C). Spermine therefore exhibited greater DNA-protecting activity than spermidine. Since the gel mobility of plasmid DNA was slightly retarded at higher concentrations (e.g., 5 and 10 mM) of polyamines, we speculate that DNA-bound polyamines repelled the drug complex from the plasmid DNA, leading to lower levels of DNA cleavage in addition to the radical scavenging effects exerted by the polyamines.

Effects of Polyamine Depletion on the Viability of $(Mith)_2$−Co(II)-Treated A549 Lung Cancer Cells. We showed that polyamines influenced the DNA binding and cleaving activities of $(Mith)_2$−Co(II), possibly weakening the action of the drug complex on cancer cells. In order to evaluate the effects of polyamines on the application of $(Mith)_2$−Co(II) to cancer therapy, the cytotoxicity of $(Mith)_2$−Co(II) in the A549 lung cancer cell line in the presence and absence of MGBG, a polyamine inhibitor, was examined. Cell viability was not affected by pretreatment with MGBG alone (1 μM). The intracellular polyamine concentration was determined by thin-layer chromatography (TLC), and the intensity of polyamine dansylation was estimated to be reduced by ~15% upon treatment with 1 μM MGBG. Statistical analysis showed that cell viability was significantly decreased with increasing concentrations of $(Mith)_2$−Co(II) ($p < 0.001$) (Figure 7). Moreover, the presence of MGBG enhanced the cytoxicity of $(Mith)_2$−Co(II) at various concentrations in the A549 lung cancer cell line ($F = 22.44$, $p < 0.001$). This result implies that depleting intracellular polyamine contents could have increased the sensitivity of cancer cells to $(Mith)_2$−Co(II).

DISCUSSION

Numerous DNA-binding metalloantibiotics, which require metal ions to maintain proper structures and function, have been developed as potential candidates for anticancer therapy (*27*). Metal ions(II) have been shown to be necessary for dimer formation of aureolic family drugs prior to binding a GC-rich DNA duplex (*20*). Recently, we have focused on the development of metal-derived complexes of the aureolic family of drugs, such as $(Chro)_2$−Fe(II) and $(Mith)_2$−Fe(II), and the exploration of their multifunctional anticancer activities, including DNA cleavage activity and topoisomerase I inhibition (*18*, *19*). Polyamines are capable of forming complexes with metal ions, including Ni(II), Co(II), Fe(II), and Cu(II) (*26*, *32*). $(Mith)_2$−Fe(II) was identified to maintain a stable dimeric conformation in the cytosol (*18*). However, our current *in vitro* studies using CD spectra suggest that higher concentrations of polyamines (e.g., 6 mM) destroyed the structural integrity of the drug complex by interacting with Fe(II). The unexpected interaction between Fe(II) and polyamines may cause the enhancement of metal-induced toxicity and carcinogenicity via modifications of DNA

Table 1: Binding Parameters between $(Mith)_2$−Co(II) and Hairpin DNA in the Presence of Polyamines at Various Concentrations

polyamines	k_a (M^{-1} s^{-1})	k_d (s^{-1})	K_a (M^{-1})[a]
buffer	$(1.56 \pm 0.18) \times 10^4$	$(6.95 \pm 0.63) \times 10^{-2}$	$(2.24 \pm 0.23) \times 10^5$
1 mM spermidine	$(1.45 \pm 0.21) \times 10^4$	$(6.40 \pm 0.65) \times 10^{-2}$	$(2.26 \pm 0.19) \times 10^5$
6 mM spermine	$(1.69 \pm 0.16) \times 10^4$	$(6.76 \pm 0.77) \times 10^{-2}$	$(2.50 \pm 0.28) \times 10^5$
1 mM spermidine	$(5.29 \pm 0.52) \times 10^3$	$(6.16 \pm 0.56) \times 10^{-2}$	$(8.58 \pm 1.01) \times 10^4$
6 mM spermine	$(3.16 \pm 0.42) \times 10^3$	$(5.88 \pm 0.52) \times 10^{-2}$	$(5.37 \pm 0.62) \times 10^4$

[a] K_a values obtained from k_a divided by k_d.

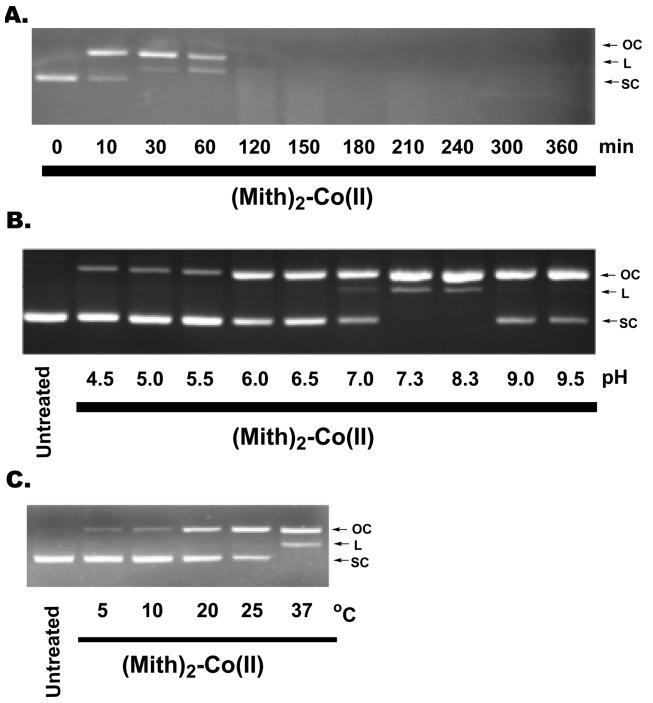

FIGURE 5: (A) Plasmid DNA was treated with $(Mith)_2$−Co(II) (10 μM) in the presence of H_2O_2 at various time points (0−360 min) at 37 °C. (B) Plasmid DNA was treated with $(Mith)_2$−Co(II) (10 μM) in the presence of H_2O_2 at various pH values (4.5−9.5) at 37 °C for 30 min. (C) Plasmid DNA was treated with $(Mith)_2$−Co(II) (10 μM) in the presence of H_2O_2 at various temperatures (5−37 °C) for 30 min. Supercoiled, open circular, and linear forms are denoted by SC, OC, and L, respectively.

bases, enhanced lipid peroxidation, and altered calcium and sulfhydryl homeostasis (*33*, *34*). In this study, the Co(II)-mediated dimeric Mith complex was shown to be more resistant to polyamine competition when compared to its Fe(II)-mediated counterpart. Therefore, we propose that $(Mith)_2$−Co(II) is able to retain its dimeric structure in the nucleus, which could potentially provide anticancer utility in clinical trials.

The interactions of cationic polyamines with negatively charged phosphate groups of nucleic acids by means of non-specific electrostatic bonds are considered to have great biological significance. Such interactions could permit conformational changes in DNA structure, condensation of DNA and chromatin, and modulation of various aspects of gene transcription by affecting the interactions of DNA-binding proteins with nucleic acids (*35*, *36*). Until now, the effects of polyamines on the DNA-reactive properties of DNA-binding anticancer drugs were poorly understood. Previous studies have shown that polyamines span both the major and minor grooves of DNA duplexes with interstrand attachments (*37*). The binding of polyamines with a DNA duplex may result in the formation of a steric barrier that blocks the access of the DNA-binding drug complex to the major

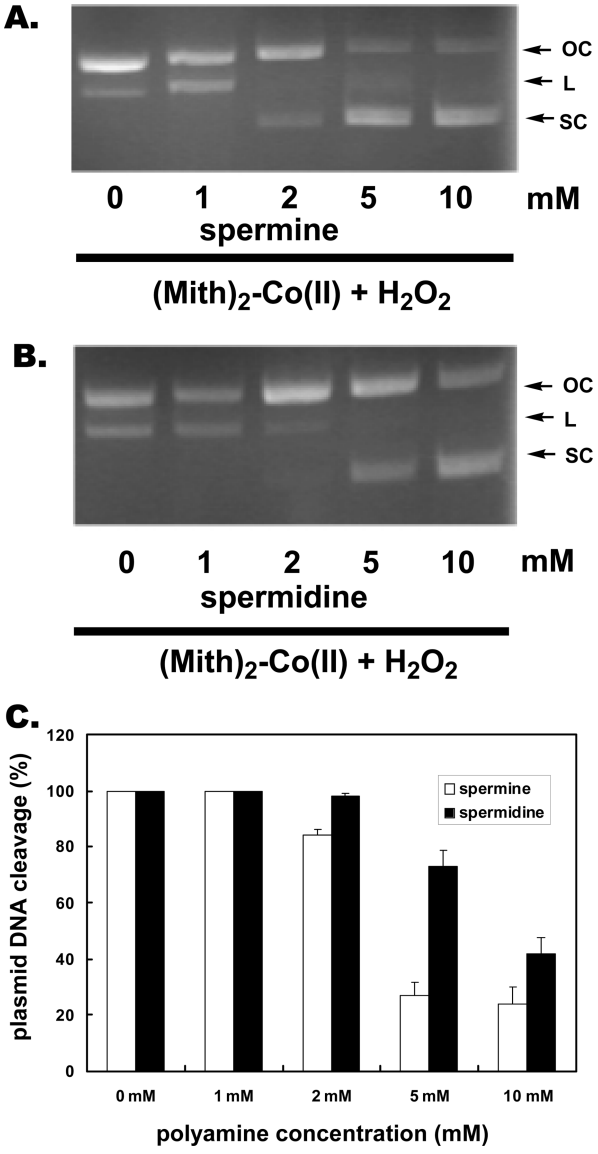

FIGURE 6: Plasmid DNA was treated with $(Mith)_2$−Co(II) (10 μM) and H_2O_2 in the presence of spermine (A) and spermidine (B) at various concentrations (0, 1, 2, 5, and 10 mM) at 37 °C for 30 min. Supercoiled, open circular, and linear forms are denoted by SC, OC, and L, respectively. (C) Quantification of percentage of plasmid cleavage relative to plasmid DNA per lane in the presence of spermine and spermidine at various concentrations (0, 1, 2, 5, and 10 mM).

and minor grooves of DNA (*36*). In the current study, $(Mith)_2$−Co(II) was shown to bind to DNA-containing GC-rich regions so rapidly at low polyamine concentrations that the association rates were nearly the same as when there was no polyamine present. The negligible influence of low concentrations of polyamines on the binding affinity of $(Mith)_2$−Co(II) is most likely due to the previous observation that polyamines preferentially

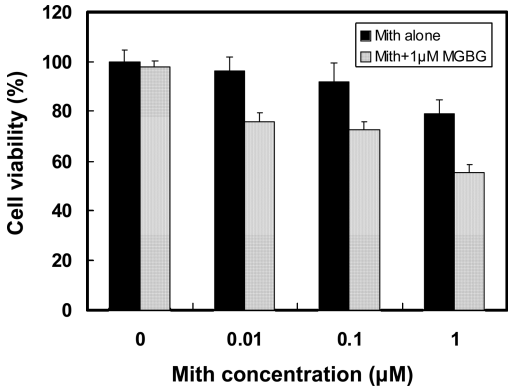

FIGURE 7: Effects of $(Mith)_2$−Co(II) at various concentrations (0−1 μM) on the viability of A549 lung cancer cells in the absence or presence of 1 μM methylglyoxal bis(guanylhydrazone) (MGBG) with a pretreatment of 24 h.

bind to the major grooves rather than the minor grooves to which $(Mith)_2$−Co(II) binds (*11*). At high polyamine concentrations, they begin to span the minor grooves; our SPR results showed that the binding affinity of $(Mith)_2$−Co(II) to hairpin DNA duplexes was attenuated by polyamines. To further understand the kinetic behavior of $(Mith)_2$−Co(II) bound to DNA, we analyzed the SPR association and dissociation phases between the drug and DNA hairpins. According to our previous findings, the association phase mainly reflects the entry of drugs into the DNA grooves, while the dissociation phase measures the hydrogen-bonding environment within the groove that accommodates the drugs (*19*). Higher concentrations of polyamines (6 mM) significantly decreased the rates of association between $(Mith)_2$−Co(II) and DNA duplexes, while the dissociation of $(Mith)_2$−Co(II) from DNA duplexes was not affected by polyamines at various concentrations. These results suggest that polyamines interfere with $(Mith)_2$−Co(II) access to the minor groove but do not affect the hydrogen bonding between the drug and DNA.

The present study provides evidence that $(Mith)_2$−Co(II) was able to induce single-stranded DNA damage in the presence of H_2O_2 via a Fenton-type reaction and also showed higher DNA cleavage activity as compared to $(Mith)_2$−Fe(II), which was studied previously. (*18*). $(Mith)_2$−Co(II) exhibited the highest oxidative activity under physiological conditions (pH 7.3 and 37 °C). Khan et al. first proposed that polyamines were capable of protecting DNA from ROS damage by quenching chemically generated singlet oxygen (*32*). In the current study, either spermine or spermidine was able to inhibit the DNA cleavage activity of $(Mith)_2$−Co(II), with spermine appearing to be more effective. Based on previous studies, two protective mechanisms of polyamines against DNA damage by $(Mith)_2$−Co(II) can be proposed (*21*, *36*). First, the binding of polyamines with DNA could lead to a conformational change in the DNA, resulting in a reduced susceptibility to binding by drug complexes and reactive hydroxyl radical attack. Second, polyamines might scavenge free radical species directly produced by $(Mith)_2$−Co(II).

Previous studies have also shown that depletion of intracellular polyamines may enhance either the efficacy of radiation therapy or the susceptibility of normal cells to oxidative stress (*23*). To analyze the effect of polyamines on the intracellular action of $(Mith)_2$−Co(II) in cancer cells, the intracellular polyamine content of the lung cancer cell line A549 was reduced by MGBG pretreatment for 24 h, followed by the addition of $(Mith)_2$−Co(II). MGBG has been clinically applied as a potent competitive inhibitor of *S*-adenosylmethionine decarboxylase in order to decrease the spermidine and spermine content of cancer cells (*38*). Here, we found that, in the presence of MGBG, $(Mith)_2$−Co(II) showed more potential antitumor activity (higher toxicity in tumor cells), suggesting that polyamine depletion rendered cancer cellular DNA susceptible to attack by the drug complex. Previous studies usually used DFMO, an irreversible inhibitor of ornithine decarboxylase, an enzyme required during the synthesis of polyamines, to decrease the polyamine content of the cancer cells (*39*). DFMO only decreases putrescine and spermidine content in the cell; spermine content is often unaffected (*5*). Previous studies indicated that putrescine and spermidine were unable to recapitulate the DNA-protective role of spermine (*40*).

The present study showed that polyamines could interfere with the actions of $(Mith)_2$−Co(II) toward DNA, including DNA binding and DNA cleavage. Several popular clinical anticancer drugs form noncovalent complexes with DNA via either intercalation (e.g., daunorubicin and actinomycin D) or groove binding (e.g., distamycin A) (*29*). Other drugs such as bleomycin bind to DNA and subsequently cause DNA backbone breakage via the redox-cycling reaction of the metal ion (*41*). The high polyamine concentration, and the subsequent DNA-protecting activity in cancer cell nuclei, may decrease the antitumor activity of these DNA-reactive anticancer drugs. Unlike previous findings that inhibiting polyamine synthesis disrupts the action of oncogenes (*5*), we determined that polyamine depletion could enhance the cytotoxicity of $(Mith)_2$−Co(II), suggesting a novel anticancer mechanism for common DNA-binding drugs through polyamine depletion.

ACKNOWLEDGMENT

We thank Drs. Andrew H.-J. Wang and Lou-Sing Kan (Academia Sinica) for help in making this research possible. The manuscript was edited by American Journal Expert (AJE).

SUPPORTING INFORMATION AVAILABLE

Polyamines at 6 mM completely abolished the DNA binding capacity of $(Mith)_2$−Fe(II) (Figure S1). Polyamines protected the plasmid against the cleavage of $(Mith)_2$−Fe(II) and the appearance of several retarded DNA bands on the gel in the presence of spermine, suggesting the occurrence of DNA condensation under this condition (Figure S2). This material is available free of charge via the Internet at http://pubs.acs.org.

REFERENCES

1. Tabor, C. W., and Tabor, H. (1984) Polyamines. *Annu. Rev. Biochem. 53*, 749–790.
2. Kusano, T., Berberich, T., Tateda, C., and Takahashi, Y. (2008) Polyamines: essential factors for growth and survival. *Planta 228*, 367–381.
3. Bachrach, U. (2004) Polyamines and cancer: minireview article. *Amino Acids 26*, 307–309.
4. Schipper, R. G., Romijn, J. C., Cuijpers, V. M., and Verhofstad, A. A. (2003) Polyamines and prostatic cancer. *Biochem. Soc. Trans. 31*, 375–380.
5. Casero, R. A.Jr., and Marton, L. J. (2007) Targeting polyamine metabolism and function in cancer and other hyperproliferative diseases. *Nat. Rev. Drug Discov. 6*, 373–390.
6. Panagiotidis, C. A., Artandi, S., Calame, K., and Silverstein, S. J. (1995) Polyamines alter sequence-specific DNA-protein interactions. *Nucleic Acids Res. 23*, 1800–1809.
7. Xiao, L., Rao, J. N., Zou, T., Liu, L., Marasa, B. S., Chen, J., Turner, D. J., Zhou, H., Gorospe, M., and Wang, J. Y. (2007) Polyamines regulate the stability of activating transcription factor-2

mRNA through RNA-binding protein HuR in intestinal epithelial cells. *Mol. Biol. Cell 18*, 4579–4590.
8. Tari, L. W., and Secco, A. S. (1995) Base-pair opening and spermine binding—B-DNA features displayed in the crystal structure of a gal operon fragment: implications for protein-DNA recognition. *Nucleic Acids Res. 23*, 2065–2073.
9. Jain, S., Zon, G., and Sundaralingam, M. (1989) Base only binding of spermine in the deep groove of the A-DNA octamer d(GTGTACAC). *Biochemistry 28*, 2360–2364.
10. Egli, M., Tereshko, V., Teplova, M., Minasov, G., Joachimiak, A., Sanishvili, R., Weeks, C. M., Miller, R., Maier, M. A., An, H., Dan Cook, P., and Manoharan, M. (1998) X-ray crystallographic analysis of the hydration of A- and B-form DNA at atomic resolution. *Biopolymers 48*, 234–252.
11. Hou, M. H., Lin, S. B., Yuann, J. M., Lin, W. C., Wang, A. H., and Kan Ls, L. (2001) Effects of polyamines on the thermal stability and formation kinetics of DNA duplexes with abnormal structure. *Nucleic Acids Res. 29*, 5121–5128.
12. Slavik, M., and Carter, S. K. (1975) Chromomycin A3, mithramycin, and olivomycin: antitumor antibiotics of related structure. *Adv. Pharmacol. Chemother. 12*, 1–30.
13. Du Priest, R. W.Jr., and Fletcher, W. S. (1973) Chemotherapy of testicular germinal tumors. *Oncology 28*, 147–163.
14. Kennedy, B. J. (1972) Mithramycin therapy in testicular cancer. *J. Urol. 107*, 429–432.
15. Sastry, M., and Patel, D. J. (1993) Solution structure of the mithramycin dimer-DNA complex. *Biochemistry 32*, 6588–6604.
16. Keniry, M. A., Banville, D. L., Simmonds, P. M., and Shafer, R. (1993) Nuclear magnetic resonance comparison of the binding sites of mithramycin and chromomycin on the self-complementary oligonucleotide d(ACCCGGGT)$_2$. Evidence that the saccharide chains have a role in sequence specificity. *J. Mol. Biol. 231*, 753–767.
17. Yarbro, J. W., Kennedy, B. J., and Barnum, C. P. (1966) Mithramycin inhibition of ribonucleic acid synthesis. *Cancer Res. 26*, 36–39.
18. Hou, M. H., and Wang, A. H. (2005) Mithramycin forms a stable dimeric complex by chelating with Fe(II): DNA-interacting characteristics, cellular permeation and cytotoxicity. *Nucleic Acids Res. 33*, 1352–1361.
19. Hou, M. H., Lu, W. J., Lin, H. Y., and Yuann, J. M. (2008) Studies of sequence-specific DNA binding, DNA cleavage, and topoisomerase I inhibition by the dimeric chromomycin A3 complexed with Fe(II). *Biochemistry 47*, 5493–5502.
20. Hou, M. H., Robinson, H., Gao, Y. G., and Wang, A. H. (2004) Crystal structure of the [Mg^{2+}-(chromomycin A3)$_2$]-d(TTGGCCAA)$_2$ complex reveals GGCC binding specificity of the drug dimer chelated by a metal ion. *Nucleic Acids Res. 32*, 2214–2222.
21. Ha, H. C., Sirisoma, N. S., Kuppusamy, P., Zweier, J. L., Woster, P. M., and Casero, R. A.Jr. (1998) The natural polyamine spermine functions directly as a free radical scavenger. *Proc. Natl. Acad. Sci. U.S.A. 95*, 11140–11145.
22. Ha, H. C., Yager, J. D., Woster, P. A., and Casero, R. A.Jr. (1998) Structural specificity of polyamines and polyamine analogues in the protection of DNA from strand breaks induced by reactive oxygen species. *Biochem. Biophys. Res. Commun. 244*, 298–303.
23. Rider, J. E., Hacker, A., Mackintosh, C. A., Pegg, A. E., Woster, P. M., and Casero, R. A.Jr. (2007) Spermine and spermidine mediate protection against oxidative damage caused by hydrogen peroxide. *Amino Acids 33*, 231–240.
24. Douki, T., Bretonniere, Y., and Cadet, J. (2000) Protection against radiation-induced degradation of DNA bases by polyamines. *Radiat. Res. 153*, 29–35.
25. Newton, G. L., Aguilera, J. A., Ward, J. F., and Fahey, R. C. (1996) Polyamine-induced compaction and aggregation of DNA—a major factor in radioprotection of chromatin under physiological conditions. *Radiat. Res. 145*, 776–780.
26. Gaboriau, F., Kreder, A., Clavreul, N., Moulinoux, J. P., Delcros, J. G., and Lescoat, G. (2004) Polyamine modulation of iron uptake in CHO cells. *Biochem. Pharmacol. 67*, 1629–1637.
27. Ming, L. J. (2003) Structure and function of "metalloantibiotics". *Med. Res. Rev. 23*, 697–762.
28. Cantor, C. R., and Tinoco, I.Jr. (1965) Absorption and optical rotatory dispersion of seven trinucleoside diphosphates. *J. Mol. Biol. 13*, 65–77.
29. Hou, M. H., Robinson, H., Gao, Y. G., and Wang, A. H. (2002) Crystal structure of actinomycin D bound to the CTG triplet repeat sequences linked to neurological diseases. *Nucleic Acids Res. 30*, 4910–4917.
30. Shiraishi, H., Kataoka, M., Morita, Y., and Umemoto, J. (1993) Interactions of hydroxyl radicals with tris(hydroxymethyl)aminomethane and Good's buffers containing hydroxymethyl or hydroxyethyl residues produce formaldehyde. *Free Radical Res. Commun. 19*, 315–321.
31. Ouameur, A. A., Arakawa, H., Ahmad, R., Naoui, M., and Tajmir-Riahi, H. A. (2005) A Comparative study of Fe(II) and Fe (III) interactions with DNA duplex: major and minor grooves bindings. *DNA Cell Biol. 24*, 394–401.
32. Khan, A. U., Mei, Y. H., and Wilson, T. (1992) A proposed function for spermine and spermidine: protection of replicating DNA against damage by singlet oxygen. *Proc. Natl. Acad. Sci. U.S.A. 89*, 11426–11427.
33. Valko, M., Morris, H., and Cronin, M. T. (2005) Metals, toxicity and oxidative stress. *Curr. Med. Chem. 12*, 1161–1208.
34. Pedreno, E., Lopez-Contreras, A. J., Cremades, A., and Penafiel, R. (2005) Protecting or promoting effects of spermine on DNA strand breakage induced by iron or copper ions as a function of metal concentration. *J. Inorg. Biochem. 99*, 2074–2080.
35. D'Agostino, L., di Pietro, M., and Di Luccia, A. (2005) Nuclear aggregates of polyamines are supramolecular structures that play a crucial role in genomic DNA protection and conformation. *FEBS J. 272*, 3777–3787.
36. D'Agostino, L., and Di Luccia, A. (2002) Polyamines interact with DNA as molecular aggregates. *Eur. J. Biochem. 269*, 4317–4325.
37. Ouameur, A. A., and Tajmir-Riahi, H. A. (2004) Structural analysis of DNA interactions with biogenic polyamines and cobalt(III)hexamine studied by Fourier transform infrared and capillary electrophoresis. *J. Biol. Chem. 279*, 42041–42054.
38. Marques, M. P., Gil, F. P., Calheiros, R., Battaglia, V., Brunati, A. M., Agostinelli, E., and Toninello, A. (2008) Biological activity of antitumoural MGBG: the structural variable. *Amino Acids 34*, 555–564.
39. Ueda, A., Araie, M., and Kubota, S. (2008) Polyamine depletion induces G1 and S phase arrest in human retinoblastoma Y79 cells. *Cancer Cell Int. 8*, 2.
40. Newton, G. L., Aguilera, J. A., Ward, J. F., and Fahey, R. C. (1997) Effect of polyamine-induced compaction and aggregation of DNA on the formation of radiation-induced strand breaks: quantitative models for cellular radiation damage. *Radiat. Res. 148*, 272–284.
41. Yang, X. L., and Wang, A. H. (1999) Structural studies of atom-specific anticancer drugs acting on DNA. *Pharmacol. Ther. 83*, 181–215.